Available online at www.sciencedirect.com
ScienceDirect
Catalysis Today 130 (2008) 75–79
CATALYSIS TODAY
www.elsevier.com/locate/cattod

Role of chelating agent on the oxidic state of hydrotreating catalysts

P. Mazoyer [a,1], C. Geantet [a,*], F. Diehl [b], S. Loridant [a], M. Lacroix [a]

[a] *Institut de Recherches sur la Catalyse et l'Environnement de Lyon, IRCELYON, UMR 5256 CNRS, Université Lyon I, 2 avenue Albert Einstein, 69626 Villeurbanne Cedex, France*
[b] *IFP, IFP-Lyon, BP 3-69390 Vernaison, France*

Available online 4 September 2007

Abstract

Chelating agents enhance the catalytic properties of HDT catalysts. It was evidenced that the presence of this organic compounds delays sulfidation. In the present study, we focused on the interaction of the chelating agent with industrial CoMo on alumina HDT catalysts after impregnation with a diammonium salt of ethylenediaminetetraacetate (diA-EDTA), drying or drying and calcination. X-ray diffraction (XRD) and Raman spectroscopy characterization demonstrate the strong interaction of the chelating agent with $CoMoO_4$. After sulfidation, enhanced catalytic activities are obtained for the treated catalysts. Interaction of model $CoMoO_4$ and $CoAl_2O_4$ solids with a solution of diA-EDTA demonstrates that the chelating agent is able to solubilize Co^{2+} cations from the molybdate but not from the spinel structure.

Keywords: Hydrodesulfurization; Chelating agent; Cobalt molybdate; Raman mapping

1. Introduction

Several patents have been published claiming the favorable effect of organic additives on the activity of hydrotreating catalysts [1–3]. These additives can be classified according to two groups: surfactant-like additives or chelating agents. Concerning this later case, van Veen et al. [4] were the first to use nitrilotriacetic acid (NTA) or ethylenediaminetetraacetic acid (EDTA) to prepare different catalysts at iso-dispersion on different model carriers. They obtained a CoMo + NTA supported on alumina twice more active in thiophene HDS than the same non-treated CoMo catalyst [5]. The presence of a higher percentage of type II CoMoS phase was proposed to explain this promoting effect. With CoW sulfide systems, the organic agent seems to favor the synergy effect of cobalt with the WS_2 phase, an effect that was never observed with the cobalt and tungsten sulfidic system. In any case, the better activity of the doped catalysts was explained by a delayed sulfidation of the promotor favoring the sulfidation of molybdenum or tungsten and allowing the formation of the optimal CoMoS phase [6,7]. The promoting effect of the chelating agent is also effective in the conversion of refractory sulfur compounds such as 4,6-dimethyldibenzothiophene [8]. More recently, Hensen et al. [9,10] studied NTA addition to Mo-based catalysts and showed an increasing activity in thiophene HDS when using NTA. In this particular case of an unpromoted catalyst, the positive effect was attributed to a higher stacking of MoS_2 slabs and a lower interaction between the active phase and the carrier. In these studies, NTA-treated catalysts were sulfided without pre-calcination of the oxide form containing the organic agent and were compared to the corresponding calcined oxide form. This point is of particular importance, since several patents recently pointed out the beneficial effect of the absence of calcination of the oxide form of NiMo or CoMo type catalyst doped with phosphorus on the catalytic activity [11].

Shimizu et al. studied the role of NTA, EDTA or CyDTA (1,2 cyclohexanediamine *N*,*N*,*N*′,*N*′-tetraacetic acid) on NiMo, CoMo and NiW type catalysts [12–14]. They observed, as van Veen et al., a beneficial effect of the organic molecule on the CoMo and NiW catalysts, and on the NiMo to a lesser extent. No promotional activity was evidenced with Mo/Al_2O_3, Co/Al_2O_3, Ni/Al_2O_3 or W/Al_2O_3. They also proposed the hypothesis of a delayed sulfidation of the promoter due to the formation of a complex between the promoter and the organic molecule and a better dispersion of

* Corresponding author. Tel.: +33 4 72 44 53 36; fax: +33 4 72 44 53 99.
E-mail address: christophe.geantet@ircelyon.univ-lyon1.fr (C. Geantet).
[1] Present address: Eurecat SA, Quai Jean Jaurès, BP 45, 07800 la Voulte sur Rhône, France.

0920-5861/$ – see front matter © 2007 Elsevier B.V. All rights reserved.
doi:10.1016/j.cattod.2007.07.013

the promoter on the surface. By EXAFS measurements, they observed an increasing coordination number of Mo-Mo and Mo-S in the modified catalyst. Prins et al. also studied the effect of chelating agents on NiMo supported on silica [15–17] and alumina [18]. On silica, it appears that the formation of a complex between Ni and the chelating agent limits the carrier–promoter interaction and favors the Ni dispersion. No significant impact on Mo was observed unless high concentrations of chelating agent were used. Moreover, delayed sulfiding kinetic of the Ni is observed with chelating molecules other than ethylenediamine. With this molecule, an increasing activity is observed without any effect on the nickel sulfidation. This strongly supports the idea of a decreasing interaction between the carrier and the active phase precursor when organic chelating additives are used. Blanchard et al. [19] also thoroughly studied the influence of ethylenediamine (En) on Mo and CoMo supported on alumina. Only the Co promoted catalyst is more active when using En, whereas Mo/alumina is unchanged even at high Mo loading. En molecule seems to inhibit the formation of cobalt molybdate and Co_3O_4 to increase the cobalt dispersion. Citric acid was also used as a complexing agent for the preparation of NiMo and CoMo supported catalysts and was supposed to favor the coordination of Co atoms around MoS_2 slabs [20] or to form entities smaller than dodecatungstate with NiW catalysts [21]. It appears that the effect of chelating agents is still not completely understood. The present work aims to provide more insight into the effect of chelating agents with a calcined CoMo catalyst.

2. Experimental

2.1. Catalysts

Industrial catalysts and laboratory prepared catalysts were used in this study. The composition of the two industrial CoMo and CoMoP catalysts is reported in Table 1.

A series of CoMo catalysts (see Table 2) with an increasing Co loading was also prepared by co-impregnation of cobalt nitrate $Ni(NO_3)_2{\cdot}6H_2O$ [Aldrich Chemical] and ammonium heptamolybdate $(NH4)_6Mo_7O_{24}{\cdot}4H_2O$ [Merck]. After co-impregnation and maturation for 10 h, catalysts were oven-dried at overnight at 393 K and if necessary, calcined under a stream of air (5×10^{-3} mol/min) at 773 K during 2 h with a heating rate of 1 K min^{-1}.

All the catalysts were sulfided under H_2/H_2S (10%) in a flow reactor (6 L/h), at 723 K during 2 h and a heating rate of 5 K min^{-1}.

Table 1
Catalysts composition of industrial γ-alumina supported catalysts

Industrial catalysts	Mo loading (wt%)	Co loading (wt%)	P loading (wt%)	Specific surface area ($m^2\ g^{-1}$)
CoMo	9.3	2.3	0	210
CoMoP	11.4	3.2	2.5	149

Table 2
Composition of the $CoMo/Al_2O_3$ series with various Co/(Co + Mo) ratios

Sample	Mo loading (wt%)	Co loading (wt%)	Co/(Co + Mo) atomic ratio
Co(0.2)Mo9	8.7	1.3	0.19
Co(0.3)Mo9	8.8	2.1	0.28
Co(0.4)Mo9	8.9	3.5	0.39
Co(0.5)Mo9	9.1	5.2	0.48

2.2. Characterization techniques

Surface area was determined by N_2 adsorption at 77 K using BET equation on a home-made apparatus after degassing the catalyst samples at 673 K during 2 h. X-ray diffraction (XRD) patterns were obtained on a BRUKER diffractometer using Cu Kα radiation (λ = 1.5406 Å).

Micro-Raman mappings were achieved using a LabRam HR spectrometer (Jobin Yvon) equipped with a CCD detector. For each sample, more than 100 spectra were obtained scanning a defined area with a motorized stage. The exciting line at 514.53 nm of an Ar^+–Kr^+ RM 2018 laser (Spectra Physics) was focused on each point with a 100× objective and a power of ca. 1 mW. It was previously checked that the laser heating was negligible with such power. The spatial resolution was ca. 1 μm and positions of bands were accurate within 1 cm^{-1}.

2.3. Tetralin hydrogenation in the presence of H_2S

Catalytic activity was checked by using a model molecule test (tetralin hydrogenation in the gas phase under pressure and in the presence of H_2S) on powdered catalysts (80 < particle size < 120 μm). The hydrogenation of tetralin (1,2,3,4-tetrahydronaphthalene) was performed in a fixed-bed gas-flow microreactor at 573 K, at a constant H_2 pressure of 4.6 MPa. The total flow rate was 56 mL/min. The partial pressure of tetralin (Fluka, purity >99%) was kept constant at 6.1 kPa by using a gas-phase saturator system (corresponding flow of tetralin, 5.48×10^{-8} mol s^{-1}). The products of tetralin hydrogenation were analyzed every 30 min by gas chromatography. *Cis* and *trans* decalins were always obtained together with small amounts of naphthalene, while no detectable amounts of isomerization or cracking products were observed. The amount of catalyst (below 250 mg) was chosen in order to obtain a conversion below 15%, ensuring the validity of a differential model for the determination of the specific rates. The deactivation of the catalyst appeared always to be negligible and within the experimental errors (accuracy below 10%). The catalyst was sulfided before the test by a conventional treatment under a H_2/H_2S mixture (15 vol% H_2S) at 400 °C (5 °C/min) for 2 h at atmospheric pressure.

3. Results and discussion

Industrial CoMo and CoMoP catalysts (see Table 1) were impregnated with an aqueous solution of diammonium salt of ethylenediaminetetraacetate (diA-EDTA) with a molar ratio diA-EDTA/Mo ratio of 0.3 which is mentioned as the optimum

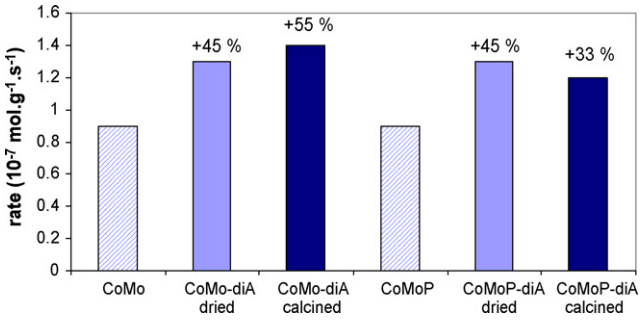

Fig. 1. Catalytic hydrogenation activity improvement of CoMo and CoMoP catalysts after impregnation with diA-EDTA and drying or calcination. (-diA: impregnated with diA-EDTA).

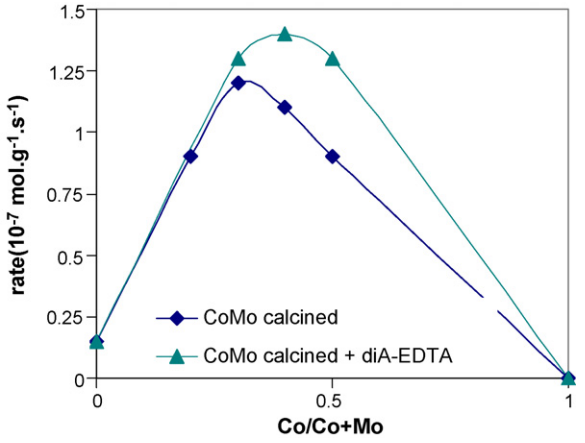

Fig. 2. Catalytic hydrogenation activity of a series of CoMo catalysts with various Co/(Co + Mo) ratio and the same catalyst impregnated with diA-EDTA and dried.

in patent literature [3]. Then, catalysts were either dried or dried and calcined at 773 K. At this calcination temperature, the chelating agent is decomposed [22]. Fig. 1 illustrates the catalytic enhancement observed in tetralin conversion either on dried or dried and calcined samples.

Fig. 1 demonstrates that even after a calcination of the impregnated catalysts a strong promoting effect is observed in contrast with the effect of a non-chelating agent which does not give any promotion after calcination. This suggests that a strong interaction already occurred in the oxide state. Thus, a series of CoMo catalysts with an increasing Co loading was prepared. The composition of this series is described in Table 2. After sulfidation of these catalysts and as it is usually observed [23], an optimum of activity was observed for a Co/(Co + Mo) atomic ratio close to 0.3 (see Fig. 2). Then, the samples were impregnated with a solution of diA-EDTA and after drying and sulfidation; we observed that the catalytic activity was significantly improved and that the maximum of activity was shifted to 0.4, suggesting that more Co atoms were involved in CoMoS active structure than previously. In fact, after calcination, XRD patterns revealed that $CoMoO_4$ content increases with Co loading (see Fig. 3) and $CoMoO_4$ is not a good promoter for CoMoS-type structures [24]. This trend was also observed by Raman spectroscopy. After impregnation with a solution of diA-EDTA, XRD patterns did not show anymore the presence of crystalline $CoMoO_4$ entities on the surface of the alumina. This evidences that the chelating agent consumes this ternary oxide undesired phase and redistributes Co^{2+} cations on the surface. Micro-Raman spectroscopy is much more sensitive to the presence of $CoMoO_4$ crystalline phase than XRD. The previously tested industrial CoMo catalyst (Fig. 1), which did not show any strong contribution of $CoMoO_4$ by XRD, was studied by Raman spectroscopy together with the diA-EDTA impregnated sample. Raman mappings of the industrial CoMo catalyst and of this sample promoted by diA-EDTA addition were recorded to get statistical information. Fig. 4 presents the average spectra obtained from 108 characterized points for each sample. The bands observed at 952, 941, 823, 335 cm^{-1} for the industrial catalyst (Fig. 4a) revealed the presence of the β-$CoMoO_4$ crystalline phase with space group *C*2/*m* [25]. The primitive cell of this phase contains four Mo^{6+} cations in C_2 and C_s sites (2 cations/site). A factor group analysis indicates there are two Raman active modes with A_g symmetry that can be assimilated to $\nu_1(MoO_4)$ vibrations. The two thin bands observed at 952 and 941 cm^{-1} correspond to these modes. The bands at 823 and 335 cm^{-1} can be assimilated to $\nu_3(MoO_4)$ and $\nu_2(MoO_4)$ vibrations, respectively. The image of the Raman intensity of the band at 823 cm^{-1} (Fig. 5a) evidences that this phase was

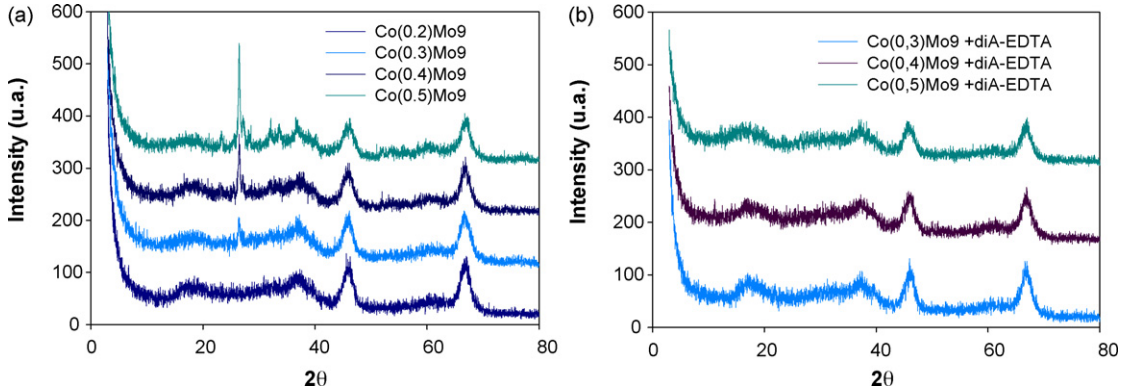

Fig. 3. XRD diffraction patterns of the series of CoMo catalyst with various Co/(Co + Mo) after calcination at 773 K (a), after impregnation with diA-EDTA and drying (b).

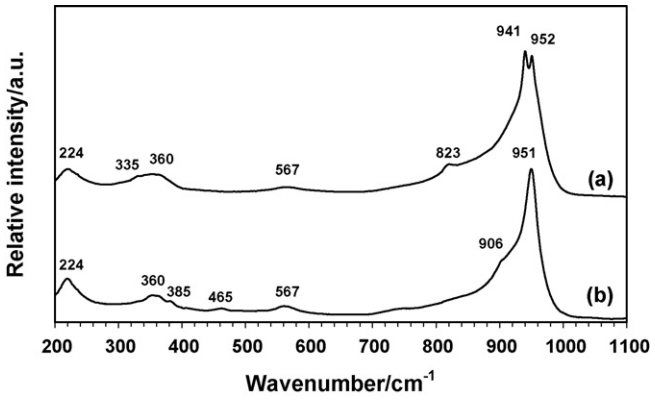

Fig. 4. Average Raman spectra of a CoMo industrial catalyst (a) and of the same catalyst impregnated with diA-EDTA (diA-EDTA/Mo molar ratio of 0.3) and dried.

observed on each examined point with a rather high intensity. However, the Raman spectrum of the industrial catalyst cannot be explained only by the presence of β-$CoMoO_4$. Indeed, the small broad band observed at 567 cm^{-1} is due to another species that could be $AlMo_6$ [26,27] or $CoMo_6$ [28] Anderson anions. The main Raman band of these anions corresponding to ν_s(Mo═O) stretching vibrations is located near 945–950 cm^{-1} and therefore could be hidden by the intense doublet at 941–952 cm^{-1} of β-$CoMoO_4$.

When the sample was treated with an aqueous solution of diA-EDTA with a diA-EDTA/Mo molar ratio of 0.3 and dried, the presence of the β-$CoMoO_4$ phase was not evidenced anymore. Indeed, the Raman image plotted in Fig. 5b clearly shows the absence of this phase in the overall examined area. The average Raman spectrum of the sample (Fig. 4b) contained bands at 951, 906, 567, 385, 360 and 224 cm^{-1} that could be due to $AlMo_6$ Anderson anions [26,27] or $CoMo_6$ [28] The intensity of these bands was almost constant in all the examined area.

Again, these experiments clearly demonstrate that the chelating agent renders soluble the $CoMoO_4$ crystalline phase. Finally, a small band was observed around 465 cm^{-1} that could correspond to $\nu(Co^{2+}–N)$ stretching vibrations and reveal complexation of some dissolved Co^{2+} cations by diA-EDTA [29]. However, one cannot exclude that some dissolved Co^{2+} cations would become counter-ions of the Anderson anions.

Then, we checked if the interaction of the chelating agent is selective to the $CoMoO_4$ phase or can also modify the distribution of Co atoms in strong interaction with the support under $CoAl_2O_4$ form. Two reference solids $CoMoO_4$ and $CoAl_2O_4$, with, respectively, 21 and 117 $m^2\ g^{-1}$ of specific

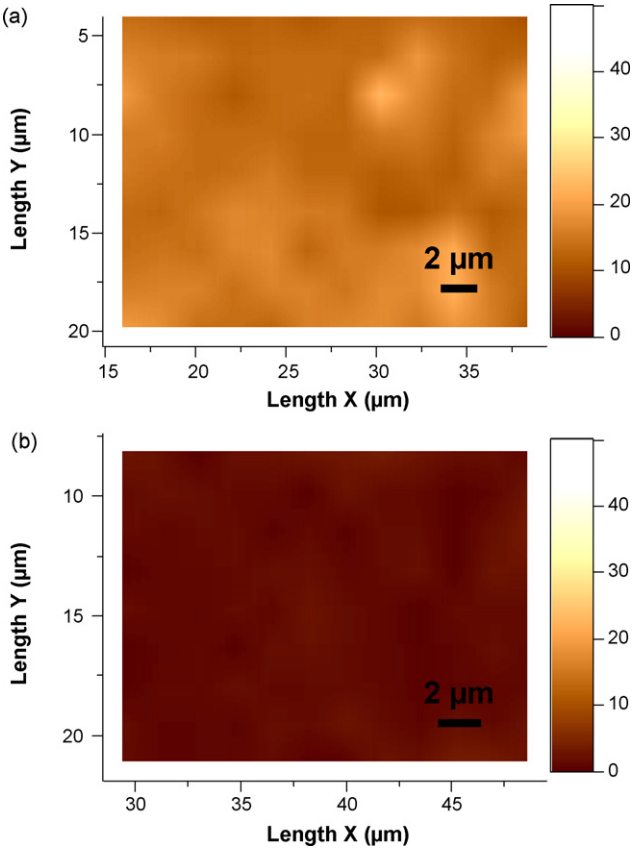

Fig. 5. Raman images of the spatial distribution of β-$CoMoO_4$ in a CoMo industrial catalyst (a) and in the same catalyst impregnated with diA-EDTA (diA-EDTA/Mo molar ratio of 0.3) and dried. These images were obtained from the relative intensity at 823 cm^{-1}.

surface area, were contacted with a solution of diA-EDTA (same concentration as before) and the amount of Co in solution was determined after 7 days. Table 3 summarizes the quantity of Co which has been dissolved. A blank experiment with only water was performed for comparison. It can be noticed that after 7 days of contact with $CoMoO_4$ more than 60% of Co was dissolved whereas only 5% of Mo is extracted. On the contrary, only 1% of Co was extracted from $CoAl_2O_4$ evidencing the strong selectivity of diA-EDTA with respect to $CoMoO_4$. The specificity of the chelating agent with respect to $CoMoO_4$ can be attributed to the different nature of the two solids. $CoMoO_4$, which can be obtained by precipitation of a Co salt and ammonium paramolybdate, can be considered as a salt with a very weak dissociation constant in water. However, in the presence of a chelating agent, this equilibrium rapidly shifts to dissolution due to the strong complexation of Co^{2+} ion in the

Table 3
Theoretical concentration of elements that can be dissolved and measured concentrations after 7 days of contact at room temperature (295 K).

	Co initial[a] (mol L^{-1})	Co (mol L^{-1})	Co extracted (%)	Mo (or Al) initial[a] (mol L^{-1})	Mo (or Al) (mol L^{-1})	Mo or (Al) extracted (%)
$CoMoO_4 + H_2O$	0.46	0.02	4	0.46	0.03	7
$CoMoO_4$ + diA-EDTA	0.46	0.29	64	0.46	0.03	5
$CoAl_2O_4 + H_2O$	0.57	0	0	1.14	0	0
$CoAl_2O_4$ + diA-EDTA	0.57	0.004	1	1.14	0.041	4

[a] Calculated concentrations for a complete dissolution of the sample.

solution by diA-EDTA. On the contrary, Co^{2+} is much more strongly bonded in the spinel structure $CoAl_2O_4$ (tetrahedral site with shorter Co–O bonds instead of octahedral and longer bonds in $CoMoO_4$) and virtually does not interact with water.

4. Conclusion

It is generally considered that a chelating agent delays the sulfidation of Co or Ni promoting atoms leading to a more efficient promotion. The chelating agent is usually introduced during the impregnation of the active elements on the support complexing in solution the doping element. In the present study, the chelating agent was impregnated on a calcined catalyst. XRD as well as Raman spectroscopy characterizations clearly demonstrate that the chelating agent consumes the undesired $CoMoO_4$ crystalline phase and thus disperse Co^{2+} cations on the surface of the catalyst in a better way to promote CoMoS phase after sulfidation. Even after calcination, a catalyst impregnated by a chelating agent such as diA-EDTA presents an improved catalytic activity; this is not what is observed when the chelating agent is used during the impregnation of the active phase precursors [30]. Thus, the use a chelating agent is an efficient method to improve catalytic activities of solids which already contain $CoMoO_4$ entities. The delaying effect of the kinetic of sulfidation is a second order effect due to the formation of new dispersed oxide entities, some of them being in interaction with the chelating agent.

References

[1] Sumitomo Metal Mining, Patent WO 96/41848 (1996).
[2] Sumitomo Metal Mining, Patent EP 0601722A1 (1994).
[3] Cytec (Shell), Patent WO 95/31280 (1995).
[4] J.A.R. Van Veen, E. Gerkema, A.M Van der Kraan, A. Knoester, J. Chem. Soc. Chem. Commun. 22 (1987) 1684.
[5] G. Kishan, L. Coulier, J.A.R. van Veen, J.W. Niemantsverdriet, J. Catal. 200 (2001) 194.
[6] L. Coulier, V.H.J. de Beer, J.A.R. van Veen, J.W. Niemantsverdriet, J. Catal 197 (2001) 26.
[7] G. Kishan, L. Coulier, J.A.R. van Veen, J.W. Niemantsverdriet, Chem. Comm. 13 (2000) 1103.
[8] W.R. Robinson, V.H.J. de Beer, J.A.R. van Veen, J.W. Niemantsverdriet, Fuel Proc. Technol. 61 (1999) 89.
[9] E.J.M. Hensen, P.J. Koyyman, Y. van der Meer, A.M. van der Kraan, V.H.J. de Beer, J.A.R. van Veen, R.A. van Santen, J. Catal. 199 (2001) 224.
[10] E.J.M. Hensen, A.M. van der Kraan, V.H.J. de Beer, J.A.R. van Veen, R.A. van Santen, Catal. Lett. 84 (2002) 59.
[11] Shell Oil Co., Patent WO 00/47321 (2000),
Patent WO 02/32572 (2002),
Patent US 6,290,841 (2001),
Patent US 6,281,158 (2001),
Patent US 6,218,333 (2001)
[12] K. Hiroshima, T. Mochizuki, T. Honma, T. Shimizu, M. Yamada, Appl. Surf. Sci. 121/122 (1997) 433.
[13] T. Shimizu, K. Hiroshima, T. Mochizuki, Honma, M. Yamada, Catal. Today 45 (1998) 271.
[14] Y. Ohta, T. Shimizu, T. Honma, M. Yamada, Stud. Surf. Sci. Catal. 127 (1999) 161.
[15] L. Medici, R. Prins, J. Catal. 163 (1996) 38.
[16] R. Cattaneo, T. Shido, R. Prins, J. Catal. 185 (1999) 199.
[17] R. Cattaneo, T. Weber, T. Shido, R. Prins, J. Catal. 191 (2000) 225.
[18] R. Cattaneo, T. Shido, R. Prins, J. Sync. Rad. 8 (2001) 158.
[19] P. Blanchard, C. Mauchaussé, E. Payen, J. Grimblot, Stud. Surf., Sci. Catal. 91 (1995) 1037.
[20] Y. Yoshimura, N. Matsubayashi, T. Sato, H. Shimada, A. Nishijima, Appl. Catal. A 79 (1991) 145.
[21] Y. Yoshimura, T. Sato, H. Shimada, N. Matsubayashi, M. Imamura, A. Nishijima, M. Higo, S. Yoshitomi, Catal. Today 29 (1996) 221.
[22] A.R. Fiorucci, L.M. Sarn, E.T.G. Cavalheiro, E.A.N. Neves, Thermochim. Acta 356 (2000) 71.
[23] M. Boudart, J.S. Arrieta, R. Della Betta, J. Am. Chem. Soc. 105 (1983) 6501.
[24] B.S. Clausen, H. Topsøe, F.E. Massoth, in: J.R. Anderson, M. Boudart (Eds.), Catalysis Science and Technology, vol. 11, Springer-Verlag, Berlin, 1996, p. 80.
[25] S.S. Saleem, Infrared Phys. 27 (5) (1987) 309.
[26] X. Carrier, J.F. Lambert, M. Che, J. Am. Chem. Soc. 119 (1997) 10137.
[27] L. Le Bihan, P. Blanchard, M. Fournier, J. Grimblot, E. Payen, J. Chem. Soc., Faraday Trans. 94 (1998) 937.
[28] C. Martin, C. Lamonier, M. Fournier, O. Mentré, V. Harlé, D. Guillaume, E. Payen, Inorg. Chem. 43 (2004) 4636.
[29] E. Faulques, D.L. Perry, S. Lott, J.D. Zubkowski, E.J. Valente, Spectrochim. Acta Part A 54 (1998) 869–878.
[30] M.S. Rana, J. Ramirez, A. Gutierrez-Alejandre, J. Ancheyta, L. Cedeno, S.K. Maity, J. Catal. 246 (2007) 100.